

1    **Reconstruction of the murine extrahepatic biliary tree using primary**  
2    **human extrahepatic cholangiocyte organoids.**

3

4    Fotios Sampaziotis<sup>1,2,3</sup>, Alexander W Justin<sup>4</sup>, Olivia C. Tysoe<sup>1,2</sup>, Stephen  
5    Sawiak<sup>5†</sup>, Edmund M Godfrey<sup>6†</sup>, Sara S Upponi<sup>6†</sup>, Richard L. Gieseck III<sup>7</sup>,  
6    Miguel Cardoso de Brito<sup>1,2</sup>, Natalie Lie Berntsen<sup>8</sup>, María J Gómez-Vázquez<sup>9</sup>,  
7    Daniel Ortmann<sup>1,2</sup>, Loukia Yiangou<sup>1,10,11</sup>, Alexander Ross<sup>1,12,13</sup>, Johannes  
8    Bargehr<sup>1,10,11,14</sup>, Alessandro Bertero<sup>1,2</sup>, Mariëlle CF Zonneveld<sup>1</sup>, Marianne T  
9    Pedersen<sup>15</sup>, Matthias Pawlowski<sup>1</sup>, Laura Valestrand<sup>8</sup>, Pedro Madrigal<sup>1,16</sup>,  
10    Nikitas Georgakopoulos<sup>2</sup>, Negar Pirmadjid<sup>2</sup>, Gregor M Skeldon<sup>17,18</sup>, John  
11    Casey<sup>19</sup>, Wenmiao Shu<sup>17,18</sup>, Paulina M Materek<sup>20</sup>, Kirsten E Snijders<sup>1</sup>,  
12    Stephanie E Brown<sup>1,2</sup>, Casey A Rimland<sup>1,2,7,21</sup>, Ingrid Simonic<sup>22</sup>, Susan E  
13    Davies<sup>23</sup>, Kim B Jensen<sup>15</sup>, Matthias Zilbauer<sup>10,12,13</sup>, William TH Gelson<sup>3</sup>,  
14    Graeme Alexander<sup>11</sup>, Sanjay Sinha<sup>1,14</sup>, Nicholas RF Hannan<sup>24,25</sup>, Thomas A  
15    Wynn<sup>7</sup>, Tom H Karlsen<sup>8</sup>, Espen Melum<sup>8</sup>, Athina E. Markaki<sup>4</sup>, Kourosh Saeb-  
16    Parsy<sup>2\*</sup>, Ludovic Vallier<sup>1,2,10,16\*</sup>

17

18    <sup>1</sup>Wellcome Trust-Medical Research Council Stem Cell Institute, Cambridge  
19    Stem Cell Institute, Anne McLaren Laboratory, University of Cambridge,  
20    Cambridge, UK

21    <sup>2</sup>Department of Surgery, University of Cambridge and NIHR Cambridge  
22    Biomedical Research Centre, Cambridge, UK

23    <sup>3</sup>Department of Hepatology, Cambridge University Hospitals NHS Foundation  
24    Trust, Cambridge, UK

- 1 <sup>4</sup>Department of Engineering, University of Cambridge, Cambridge, UK
- 2 <sup>5</sup>Department of Clinical Neurosciences, University of Cambridge, Cambridge,  
3 UK
- 4 <sup>6</sup>Department of Radiology, Cambridge University Hospitals NHS Foundation  
5 Trust, Cambridge, UK
- 6 <sup>7</sup>Immunopathogenesis Section, Laboratory of Parasitic Diseases, National  
7 Institute of Allergy and Infectious Diseases, National Institutes of Health,  
8 Bethesda, Maryland, USA
- 9 <sup>8</sup>Norwegian PSC Research Center, Department of Transplantation Medicine,  
10 Division of Surgery, Inflammatory Diseases and Transplantation, Oslo  
11 University Hospital, Rikshospitalet, Oslo.
- 12 <sup>9</sup>Cambridge Genomic Services, Department of Pathology, University of  
13 Cambridge, Cambridge, UK
- 14 <sup>10</sup>Wellcome Trust-Medical Research Council Stem Cell Institute, Cambridge  
15 Stem Cell Institute, University of Cambridge, Cambridge, UK
- 16 <sup>11</sup>Department of Medicine, School of Clinical Medicine, University of  
17 Cambridge, Cambridge, UK.
- 26 <sup>12</sup>University Department of Paediatrics, University of Cambridge, Cambridge,  
27 UK
- 28 <sup>13</sup>Department of Paediatric Gastroenterology, Hepatology and Nutrition,  
29 Cambridge University Hospitals NHS Foundation Trust, Cambridge, UK
- 30 <sup>14</sup>Division of Cardiovascular Medicine, University of Cambridge, Cambridge,  
31 UK
- 32 <sup>15</sup>Biotech Research and Innovation Centre (BRIC), University of Copenhagen,  
33 Copenhagen, Denmark

1 <sup>16</sup>Wellcome Trust Sanger Institute, Hinxton, UK

2 <sup>17</sup>School of Engineering and Physical Sciences, Heriot-Watt University, United  
3 Kingdom

4 <sup>18</sup>Department of Biomedical Engineering, University of Strathclyde, United  
5 Kingdom

6 <sup>19</sup>Department of Surgery, University of Edinburgh, Edinburgh Royal Infirmary,  
7 Edinburgh, EH16 4SU, United Kingdom

8 <sup>20</sup>NIHR Cambridge Biomedical Centre (BRC) hiPSCs core facility

9 <sup>21</sup>University of North Carolina, Chapel Hill School of Medicine, Chapel Hill,  
10 North Carolina, USA

11 <sup>22</sup>Medical Genetics Laboratories, Cambridge University Hospitals NHS Trust,  
12 Cambridge, UK

13 <sup>23</sup>Department of Histopathology, Cambridge University Hospitals NHS  
14 Foundation Trust, Cambridge, UK

15 <sup>24</sup>Center for Biomolecular Sciences, University of Nottingham, UK

16 <sup>25</sup>Nottingham Digestive Diseases Centre, National Institute for Health  
17 Research (NIHR) Nottingham Biomedical Research Centre at the Nottingham  
18 University Hospitals NHS Trust and University of Nottingham.

19

20 **Authorship note:** \* Kourosh Saeb-Parsy and \* Ludovic Vallier contributed  
21 equally to this work.

22 <sup>†</sup>Stephen Sawiak, <sup>†</sup>Edmund Godfrey and <sup>†</sup>Sara Upponi contributed equally to  
23 this work.

24 **Correspondence:** Ludovic Vallier, Laboratory for Regenerative Medicine,  
25 West Forvie Building, Robinson Way, University of Cambridge. Cambridge

1 CB2 0SZ, United Kingdom. Telephone: 44.1223.747489; Fax:  
2 44.1223.763.350; E-mail: [lv225@cam.ac.uk](mailto:lv225@cam.ac.uk).

3

4 **Keywords:** Cholangiocytes, bile duct, bio-engineering, tissue engineering,  
5 organoids, regenerative medicine, cell-based therapy, biliary atresia, PGA  
6 scaffold, collagen scaffold, densified collagen

7

## Abstract

Treatment of common bile duct disorders such as biliary atresia or ischaemic strictures is limited to liver transplantation or hepatojejunostomy due to the lack of suitable tissue for surgical reconstruction. Here, we report a novel method for the isolation and propagation of human cholangiocytes from the extrahepatic biliary tree and we explore the potential of bioengineered biliary tissue consisting of these extrahepatic cholangiocyte organoids (ECOs) and biodegradable scaffolds for transplantation and biliary reconstruction in vivo. ECOs closely correlate with primary cholangiocytes in terms of transcriptomic profile and functional properties (ALP, GGT). Following transplantation in immunocompromised mice ECOs self-organize into tubular structures expressing biliary markers (CK7). When seeded on biodegradable scaffolds, ECOs form tissue-like structures retaining biliary marker expression (CK7) and function (ALP, GGT). This bioengineered tissue can reconstruct the wall of the biliary tree (gallbladder) and rescue and extrahepatic biliary injury mouse model following transplantation. Furthermore, it can be fashioned into bioengineered ducts and replace the native common bile duct of immunocompromised mice, with no evidence of cholestasis or lumen occlusion up to one month after reconstruction. In conclusion, ECOs can successfully reconstruct the biliary tree following transplantation, providing proof-of-principle for organ regeneration using human primary cells expanded in vitro.

1 Disorders of the extrahepatic bile ducts carry considerable morbidity and  
2 mortality. Indeed, 70% of pediatric liver transplantations are performed to treat  
3 biliary atresia<sup>1</sup>, Primary Sclerosing Cholangitis (PSC) alone accounts for 5%  
4 of US liver transplantations<sup>2</sup> and biliary complications are the leading cause of  
5 graft failure following deceased liver transplantation<sup>3,4</sup>. Treatment options  
6 remain limited<sup>5,6</sup> due to the lack of healthy tissue that can be used to  
7 reconstruct and replace diseased bile ducts. In vitro expansion of native  
8 cholangiocytes could address this challenge and provide cells suitable for  
9 tissue engineering applications such as biliary reconstruction. However, the  
10 culture of primary biliary epithelium remains problematic<sup>7</sup>. Here we report a  
11 novel method for the isolation and propagation of primary human  
12 cholangiocytes from the extrahepatic biliary tree, compatible with regenerative  
13 medicine applications. The resulting Extrahepatic Cholangiocyte Organoids  
14 (ECOs) express key biliary markers such as Cytokeratin 7 (KRT7 or CK7),  
15 Cytokeratin 19 (KRT19 or CK19), Gamma Glutamyl-Transferase (GGT),  
16 Cystic fibrosis transmembrane conductance regulator (CFTR) and maintain  
17 their functional properties in vitro including Alkaline Phosphatase (ALP), GGT  
18 activity and responses to secretin and somatostatin. The potential of ECOs for  
19 tissue engineering and clinical applications is further illustrated by their  
20 capacity to populate biodegradable scaffolds, organize into a functional biliary  
21 epithelium and rescue a murine model of extrahepatic biliary injury (EHBI).

22

## 23 **Results**

### 24 **Human extrahepatic cholangiocytes can be propagated as organoids**

1 We first focused on identifying optimal conditions to isolate primary  
2 cholangiocytes from the biliary epithelium which forms a monolayer covering  
3 the luminal surface of the biliary tree<sup>8</sup>. We tested several approaches for  
4 recovering these cells and mechanical dissociation by brushing or scraping  
5 the bile duct lumen was associated with improved survival compared to  
6 enzymatic digestion (Figure 1a, Supplementary Fig 1a). Furthermore, the  
7 majority of the resulting cells co-expressed the biliary markers CK7 and CK19  
8 ( $94.6 \pm 2.4\%$ , SD; n=3); while no contamination from mesenchymal cell types  
9 was detected (Supplementary Fig 2). Consequently, mechanical dissociation  
10 constitutes the optimal method for harvesting extrahepatic cholangiocytes.

11 To discern appropriate conditions for the maintenance and propagation of  
12 these cells, we optimized our recently established system for 3D culture of  
13 human induced pluripotent stem cell-derived intrahepatic cholangiocytes<sup>9,10</sup>.  
14 Screening of multiple growth factors known to support expansion of  
15 cholangiocytes and epithelial organoids<sup>11,12</sup> (Supplementary Fig 1b-1c)  
16 identified that the combination of Epidermal Growth Factor (EGF), R-spondin  
17 and Dickkopf-related protein 1 (DKK-1) promoted the growth of primary  
18 cholangiocytes into organoids (Supplementary Fig 3a, 3b). Due to the  
19 paradoxical requirement for both a Wnt potentiator (R-spondin) and an  
20 inhibitor (DKK-1), we characterized the canonical and non-canonical/PCP Wnt  
21 pathway activity in ECOs. Our results demonstrate higher  $\beta$ -catenin  
22 phosphorylation in ECOs compared to cells treated with R-spondin but no  
23 DKK-1 (Supplementary Fig 1d-1e), signifying lower WNT canonical pathway  
24 activity in these cells. Furthermore ECOs exhibit higher Rho Kinase activity  
25 compared to cells treated with R-spondin but no DKK-1 (Supplementary Fig

1 1f), which could be consistent with enhanced non-canonical/PCP signaling in  
2 ECOs. Thus, it is possible that non-canonical Wnt signaling controls ECO  
3 expansion marking a notable difference with previous organoid culture  
4 conditions<sup>12</sup>.

5 Under these conditions, we derived 8 different ECO lines (Supplementary  
6 Table 1) from a variety of deceased donors aged from 33 to 77 years.  
7 Notably, we obtained similar results by using cholangiocytes isolated from the  
8 gallbladder or by harvesting common bile duct cholangiocytes using an  
9 Endoscopic Retrograde Cholangio-Pancreatography (ERCP) brush instead of  
10 scrapping the lumen (Supplementary Fig 4). Consequently, ECOs can be  
11 derived from different areas of the extra-hepatic biliary tree and harvested  
12 using peri-operative (dissection and scrapping) or minimally invasive (ERCP  
13 brushings) approaches.

14

#### 15 **ECOs maintain key biliary markers and function in culture**

16 The resulting cells were expanded in vitro for prolonged periods of time  
17 (Supplementary Fig 5a) while maintaining their genetic stability  
18 (Supplementary Fig 5b-5c). Electron microscopy revealed the presence of  
19 characteristic ultrastructural features including cilia, microvilli and tight  
20 junctions<sup>13</sup> (Supplementary Fig 3c), while QPCR and immunofluorescence  
21 (IF) analyses established the expression of key biliary markers such as *KRT7*  
22 or *CK7*, *KRT19* or *CK19*, Hepatocyte Nuclear Factor 1 beta (*HNF1B*), *GGT*,  
23 Secretin Receptor (*SCTR*), sodium-dependent bile acid transporter  
24 (*ASBT/SLC10A2*), *CFTR* and SRY-box 9 (*SOX9*)<sup>9</sup> (Figure 1b-1c,



1 Supplementary Fig 4c-4d, 3d-3e). Of note, stem cell markers such as  
2 *POU5F1* or *OCT4*, *NANOG*, prominin 1 (*PROM1*), leucine rich repeat  
3 containing G protein-coupled receptor (*LGR*) *LGR-4/5/6*; markers of non-  
4 biliary lineages including albumin (*ALB*),  $\alpha$ 1-antitrypsin (*SERPINA1* or *A1AT*),  
5 keratin 18 (*KRT18*), pancreatic and duodenal homeobox 1 (*PDX1*), insulin  
6 (*INS*) and glucagon (*GCG*); and EMT markers (vimentin (*VIM*), snail family  
7 transcriptional repressor 1 (*SNAI1*) and S100 calcium binding protein A4  
8 (*S100A4*) were not detected (Supplementary Fig 6a-6c). On the other hand,  
9  $98.1\% \pm 0.9\%$  (SD; n=3) of the cells co-expressed CK7 and CK19 following  
10 20 passages (Supplementary Fig 2) thereby confirming the presence of a  
11 near homogeneous population of cholangiocytes.

12 Transcriptomic analyses (Figure 1d, Supplementary Fig 7, Supplementary  
13 Table 2) revealed that ECOs maintain a stable gene expression profile over  
14 multiple passages (Pearson correlation coefficient for Passage 1 (P1) vs.  
15 Passage 20 (P20)  $r=0.99$ , Supplementary Fig 7a-b), express key biliary  
16 markers (Supplementary Fig 7c) and cluster closely to freshly isolated  
17 cholangiocytes (Supplementary Fig 7d) (Pearson correlation coefficient for  
18 Primary Cholangiocytes (PCs) vs. Passage 20 (P20)  $r=0.92$ ; Supplementary  
19 Fig 7b). Gene ontology analyses confirmed enrichment of pathways  
20 characteristic for the biliary epithelium (Supplementary Fig 7e). Considered  
21 collectively, these results demonstrate that primary cholangiocytes derived  
22 from the extrahepatic biliary tree can be expanded in vitro without losing their  
23 original characteristics.

24 We then further characterized ECOs by focusing on their function following  
25 long term culture (20 passages). The biliary epithelium regulates the

1 homeostasis of bile through the transport of ions, water and bile acids<sup>8,14</sup>. The  
2 secretory capacity of ECOs was interrogated using Rhodamine-123, a  
3 fluorescent substrate for the cholangiocyte surface glycoprotein Multidrug  
4 Resistance protein-1 (MDR1)<sup>15,16</sup> (Figure 2a-2c). Rhodamine-123  
5 accumulated in the ECO lumen only in the absence of the MDR-1 antagonist  
6 verapamil, thereby confirming active secretion through MDR-1 (Figure 2a-2c).  
7 Luminal extrusion of bile acids<sup>17</sup> was also demonstrated by showing that the  
8 fluorescent bile acid Cholyl-Lysyl-Fluorescein (CLF) was actively exported  
9 from ECOs (Figure 2d-2f). Furthermore, ECO ALP and GGT activity was  
10 comparable to freshly plated primary cholangiocytes (Figure 2g-2h,  
11 Supplementary Fig 4e-4f). The response of ECOs to secretin and  
12 somatostatin was also assessed. Secretin promotes water secretion,  
13 distending the bile duct lumen, while somatostatin negates the effects of  
14 secretin<sup>18–20</sup>. Accordingly, organoids exposed to secretin increased their  
15 diameter compared to untreated controls, while somatostatin inhibited the  
16 effect of secretin (Figure 2i-2j). Our data, therefore, demonstrate that ECOs  
17 maintain their functional properties after long term culture.

18

### 19 **ECOs self-organize into tubular structures after transplantation**

20 These results prompted us to investigate the potential of ECOs for in vivo use,  
21 especially regenerative medicine applications. We first characterized the  
22 potential of ECOs for in vivo engraftment and survival by transplanting cells  
23 under the kidney capsule of NOD.Cg-Prkdc<sup>scid</sup> Il2rg<sup>tm1Wjl</sup> (NSG) mice  
24 (Supplementary Fig 8a) for 12 weeks<sup>21</sup>. ECOs successfully engrafted forming

1 tubular structures expressing biliary markers such as CK19 (Supplementary  
2 Fig 8b-d).

3 Notably, no tumour formation or markers of differentiation to other lineages  
4 were detected (Supplementary Fig 8d). Thus, ECOs appear to maintain their  
5 basic characteristics even after prolonged engraftment in vivo under the  
6 kidney capsule.

7

## 8 **ECOs populate biodegradable scaffolds**

9 To assess the potential of ECOs for tissue engineering, we first interrogated  
10 their capacity for populating Polyglycolic Acid (PGA) biodegradable scaffolds  
11 commonly used to provide the structural and mechanical support required for  
12 tissue reconstruction<sup>22</sup>. Indeed, PGA is one of the most widely used synthetic  
13 polymers since it does not induce inflammatory responses in the surrounding  
14 tissue; it is biodegradable; and it is more flexible and easier to process  
15 compared to natural polymers such as collagen<sup>23</sup>. To facilitate tracking of the  
16 cells, ECOs expressing Green Fluorescent Protein (GFP) were generated  
17 through viral transduction (Supplementary Fig. 9a-9b). The resulting cells  
18 were seeded on PGA scaffolds, attached to the PGA fibers after 24-48 hours  
19 and continued to grow for 4 weeks until the scaffold was confluent (Figure 3a-  
20 3d). Primary cholangiocytes plated in 2D conditions demonstrated limited  
21 expansion potential and failed to reach confluency when seeded on the  
22 scaffolds (Supplementary Fig 10a-b), suggesting that the proliferative capacity  
23 of ECOs is crucial for successful scaffold colonization. The populated PGA  
24 scaffolds (Figure 3b-3c), could easily be handled with forceps and divided into

1 smaller pieces with a surgical blade. Furthermore, the cells populating the  
2 scaffolds retained expression of biliary markers such as CK7 and CK19  
3 (Figure 3e-3f), demonstrated no evidence of epithelial–mesenchymal  
4 transition (EMT; Figure 3e, 3g) and maintained their functional properties  
5 including ALP and GGT activity (Figure 3h-3i). Therefore, ECOs can  
6 successfully populate PGA scaffolds, while maintaining their functionality and  
7 marker expression.

### 9 **ECO-populated scaffolds reconstruct the gallbladder wall**

10 Following these encouraging results, we decided to define the capacity of  
11 ECOs to repair the biliary epithelium. For that, we developed a mouse model  
12 of extrahepatic biliary injury (EHBI). More specifically, to simulate biliary tree  
13 wall defects requiring biliary reconstruction<sup>24</sup>, the biliary tree of healthy NSG  
14 mice was compromised through a longitudinal incision in the gallbladder wall  
15 (Figure 4a). The surgical defect in the gallbladder wall was subsequently  
16 repaired by transplanting bioengineered tissue into the injured animals, which  
17 was generated using GFP-expressing ECOs (see previous section; Figure 3).  
18 Acellular PGA scaffolds and scaffolds populated with GFP-expressing  
19 fibroblasts (Supplementary Fig 11a-11d) were used as a negative controls.  
20 Animals receiving acellular scaffolds died within 24 hours of the operation  
21 (Figure 4b) and post-mortem examination revealed yellow pigmentation of the  
22 peritoneal cavity and seminal vesicles consistent with bile leak  
23 (Supplementary Fig 12a); while all animals in the fibroblast-scaffold group  
24 failed to reconstruct their gallbladder which was replaced by fibrotic tissue

1 incompatible with bile transport or storage (Supplementary Fig 13e-13g). In  
2 contrast, animals transplanted with scaffolds containing ECOs survived for up  
3 to 104 days without complications and were culled electively (Figure 4b).  
4 Notably, the reconstructed gallbladders in the ECO group were fully  
5 remodeled resembling the morphology of their native counterparts (Figure 4c,  
6 Supplementary Fig 12b). Histology (Figure 3d), IF and QPCR analyses of the  
7 ECO-reconstructed gallbladders (Figure 3e, Supplementary Fig 14c-14d)  
8 unveiled integration of GFP-positive ECOs expressing biliary markers, such  
9 as *KRT19*, *KRT7*, *HNF1B*, *SOX9*, *CFTR* and a human-specific epitope for  
10 Ku80 (Figure 4e, Supplementary Fig 12c). Of note, these IF analyses also  
11 showed the presence of mouse mesenchymal cells expressing vimentin and  
12 endothelial cells expressing CD31 in the reconstructed biliary epithelium  
13 suggesting that the scaffold is colonized by endogenous cells after  
14 transplantation (Supplementary Fig 12c). Furthermore, we also identified a  
15 population of GFP+/vimentin+/CK19- cells, suggesting that ECOs may also  
16 contribute to the scaffold stroma in vivo; possibly through EMT  
17 (Supplementary Fig 12c, 12e). The integrity of the reconstructed gallbladder  
18 lumen and its exposure to bile through continuity with the biliary tree were  
19 demonstrated using Magnetic Resonance Cholangio-Pancreatography  
20 (MRCP) imaging prior to removal of the organ and was further confirmed with  
21 FITC cholangiograms (Figure 4f-4g, Supplementary Fig 12f, Supplementary  
22 Video 1). Post mortem surgical examination and full body Magnetic resonance  
23 Imaging 104 days post transplantation revealed no evidence of tumor  
24 formation (Supplementary Fig 12f, Supplementary Video 2) while IF analyses  
25 revealed no GFP+ cells in the adjacent liver tissue (data not shown). On the

contrary, gallbladders reconstituted with fibroblasts controls exhibited obliteration of the gallbladder lumen (Supplementary Fig 11h-11i) and replacement of the lumen and biliary epithelium by fibroblasts expressing Fibroblast Specific Antigen S100A4 (Supplementary Fig. 11i-11j). Considered collectively, our findings demonstrate the capacity of ECOs to colonize their physiological niche and regenerate part of the biliary tree without any complications.

### **ECOs on collagen scaffolds generate bioengineered bile ducts**

Reconstruction of the gallbladder wall provided proof-of-principle for the capacity of ECOs to regenerate the biliary epithelium after injury; however, the majority of extrahepatic bile duct disorders affect the common bile duct (CBD). Therefore, we focused on the generation of a tubular ECO-populated scaffold, which could be used for bile duct replacement surgery. The internal diameter of the mouse CBD is approximately 100µm with a wall thickness of less than 50µm, which precluded the use of a PGA scaffold due to mechanical properties. Instead, we generated densified collagen tubular scaffolds (Figure 5a-5b) which were populated with GFP-expressing ECOs (Figure 5c-5e). The use of densified collagen enabled the generation of constructs with an external diameter ranging from 250 to 600µm and adequate strength to maintain a patent lumen (Figure 5d). Notably, the cells populating the collagen scaffolds maintained expression of biliary markers such as *KRT19*, *KRT7*, *HNF1B*, *SOX9* and *CFTR* (Figure 5f-5g) and exhibited GGT and ALP enzymatic activity (Figure 5h-5i). Primary epithelial cells of different origin

(human mammary epithelial cells; HMEC) failed to survive and adequately populate densified collagen tubes under the same conditions (Supplementary Fig. 13a). Moreover, plated HMECs failed to survive in a 10% (vol/vol) bile solution compared to ECOs (Supplementary Fig. 13b), further confirming that ECOs constitute the only cell type capable of generating bile resistant bioengineered bile ducts. Collectively, these results demonstrate the capacity of ECOs for populating tubular densified collagen scaffolds without losing their original characteristics.

### **Bioengineered bile ducts replace the native mouse bile duct**

We then decided to explore the possibility to replace the native CBD of NSG mice with a bioengineered duct consisting of an ECO-populated densified collagen tube (Figure 5). A mid-portion of the native CBD was removed and an ECO-populated collagen tube was anastomosed end-to-end to the proximal and distal duct remnants (Figure 6a). Fibroblast populated tubes were used as a negative control. Biliary reconstruction was achieved in all animals transplanted with ECO-populated tubes (Figure 6b-6c, Supplementary Fig 14a-14d), which were followed up for up to a month post transplantation (Supplementary Fig 14d). Histology and IF and QPCR analyses (Figure 6d-6f, Supplementary Fig 14a-14b) revealed a patent lumen, with formation of a biliary epithelium by the transplanted GFP<sup>+</sup> cells (Figure 6e-6f, Supplementary Fig 14a-14b); confirmed the expression of biliary markers, such as *KRT19*, *KRT7*, *HNF1B*, *CFTR*, *SOX9* (Figure 6d, 6f, Supplementary Fig 14b) by the engrafted cells; but also illustrated the

1 presence of mouse stromal and endothelial cells (Supplementary Fig 14b).  
2 Moreover, we observed minimal apoptosis and proliferation in the  
3 transplanted tubes 1 month after transplantation, confirming the stability and  
4 integrity of the reconstituted biliary epithelium (Supplementary Fig 14b-14c).  
5 Lumen patency was further confirmed by Fluorescein Isothiocyanate (FITC)  
6 cholangiogram, MRCP and serum cholestasis marker measurements (Figure  
7 6g, Supplementary Fig 14e-14f, Supplementary video 3). Accordingly animals  
8 receiving ECO-populated tubes exhibited no elevation in serum cholestasis  
9 markers (Bilirubin, ALP; Supplementary Fig 14e) and a patent lumen on  
10 imaging (Figure 6g, Supplementary Fig 14f); while the bio-artificial common  
11 bile ducts retained their ALP activity in vivo (Figure 6h).

12 On the contrary, all fibroblast-populated collagen tubes failed due to lumen  
13 occlusion (Figure 6b-6c, 6e-6g, Supplementary Fig 14d), resulting in high  
14 biliary pressures and bile leak through the site of anastomosis (Figure 6b). In  
15 conclusion, our results demonstrate the capacity of ECO-populated collagen  
16 tubes to replace the native CBD in vivo.

17

## 18 **Discussion**

19 We have demonstrated that epithelial cells from the extrahepatic biliary tree  
20 can be expanded and propagated in vitro while maintaining their  
21 cholangiocyte transcriptional signature and functional characteristics. In  
22 addition, our results show that primary cholangiocytes expanded in vitro as  
23 organoids have a unique potential for organ regeneration. Indeed, our system  
24 provides the first proof-of-principle for the application of regenerative medicine



1 in the context of common bile duct pathology. The capacity to replace a  
2 diseased common bile duct with an in vitro bio-engineered ECO-tube could  
3 have a considerable impact for the management of disorders such as biliary  
4 atresia, which constitutes the leading cause for pediatric liver transplantation<sup>1</sup>;  
5 or ischemic strictures which are one of the most common complications  
6 following transplantation<sup>3</sup>. Consequently ECO-populated scaffolds constitute a  
7 novel system with high clinical relevance in the field of cholangiopathies.

8 Furthermore, studies of the extrahepatic biliary epithelium have been limited  
9 by technical challenges in long-term culture and large-scale expansion of  
10 primary cholangiocytes. These challenges have so far precluded large scale  
11 experiments such as transcriptomic and genome-wide analyses which are  
12 urgently needed to better understand bile duct diseases, such as PSC and  
13 cholangiocarcinoma. The capacity of ECOs for large scale expansion, could  
14 address this challenge. Indeed, we demonstrate that starting from  $10^5$   
15 extrahepatic cholangiocytes we can generate between  $10^{20}$  –  $10^{25}$  cells after  
16 20 passages. Therefore, ECOs not only represent a novel source of cells for  
17 cell based therapy but also provide a unique model system for studying the  
18 physiology and modeling disorders of the extrahepatic biliary tree in vitro.

19 Access to human tissue constitutes a considerable limitation for systems  
20 based on primary cells. However, we show that ECOs can be obtained not  
21 only from the common bile duct but also from the gallbladder. Gallbladder  
22 tissue is easily accessible and routinely discarded following liver  
23 transplantation and cholecystectomy, one of the most common surgical  
24 procedures performed. Furthermore, in individuals not having surgery the  
25 common bile duct can be accessed using minimally invasive procedures, such

1 as Endoscopic Retrograde Cholangio-Pancreatography (ERCP) and we  
2 demonstrate that cholangiocytes can be obtained through brushings, which  
3 are routinely performed to acquire histology specimens. Notably, no  
4 morphological or functional differences were observed between organoids  
5 obtained with these different methods. Moreover, due to the scalability of our  
6 system only a small amount of starting material is required. Finally, recent  
7 progress in replacing Matrigel by custom made hydrogels to grow gut  
8 organoids<sup>25</sup> suggest that translating our system from Matrigel to Good  
9 Manufacturing Practice (GMP) could be feasible. Considered together, these  
10 approaches effectively address challenges of tissue availability and open the  
11 possibility of autologous as well as allogeneic cell based therapy.

12 Notably, the derivation of primary hepatic stem cells using an organoid culture  
13 system has been reported previously<sup>12</sup>. However, the capacity of the resulting  
14 cells to differentiate into functional cholangiocytes and populate the biliary tree  
15 in vivo remains to be demonstrated. Furthermore, in vivo applications of such  
16 platforms could be restricted by contaminating stem cells with a capacity to  
17 proliferate inappropriately after transplantation and/or differentiate into non-  
18 biliary cell types. Despite the association between organoids and adult stem  
19 cells<sup>26</sup>, we never observed the expression of hepatocyte or pancreatic  
20 markers during our experiments either in vitro or after transplantation,  
21 suggesting that the differentiation capacity of ECOs is limited to their lineage  
22 of origin. Moreover, canonical WNT signaling, which is crucial for the  
23 expansion of adult stem cell organoids<sup>27</sup> is blocked in our culture conditions  
24 through the use of DKK-1 and further studies may be required to fully  
25 elucidate the role of R-spondin in our system. Considered together, these

1 observations suggest that our culture system does not include a stem cell  
2 population. However, we cannot completely exclude that these cells could  
3 represent a biliary progenitor population based on their ability to self-  
4 propagate and generate organoids from single cells.

5 Our system provides proof-of-principle for the application of primary cells in  
6 regenerative medicine; however, the use of stem cells has been suggested as  
7 an alternative for cell based therapy. Although we have recently established a  
8 system for the generation of stem cell-derived cholangiocyte-like cells  
9 (CLCs)<sup>9</sup>, there are considerable differences between ECOs and CLCs that  
10 render ECOs better suited to regenerative therapies for extrahepatic biliary  
11 injury. CLCs correspond to intrahepatic cholangiocytes, while ECOs represent  
12 extrahepatic biliary epithelium. These two cell types are distinct in terms of  
13 embryological origin and disease involvement<sup>14</sup>. Furthermore, CLCs still  
14 express fetal markers and therefore are more immature compared to ECOs  
15 derived from primary cells<sup>9</sup>. Therefore, CLCs may require a period of  
16 adjustment and further maturation in vivo, while mature, functional cells, such  
17 as ECOs, are required for coping with biliary injury in the acute setting.  
18 Finally, although hiPSCs provide a very good source of cells capable of  
19 generating almost any tissue, fully differentiated CLCs cannot be expanded;  
20 initial derivation/characterization of hiPSC lines remains time consuming;  
21 while variability in capacity of differentiation still constitutes a challenge. ECOs  
22 can be derived in less than 24 hours with a very high efficiency and can be  
23 expanded for multiple passages without losing their original characteristics.  
24 Consequently, ECOs are comparable to CLCs in terms of scalability, while

1 their mature phenotype provides a unique advantage for regenerative  
2 medicine applications in the context of tissue repair.

3 In conclusion, our results open up novel avenues for the use of extrahepatic  
4 primary biliary tissue as a novel platform for in vitro studies, disease modeling  
5 and cell based therapy applications.

6

#### 7 **Accession codes**

8 Accession number for microarray data: E-MTAB-4591.

9

#### 10 **Data availability statement**

11 The microarray data are open access and available online on ArrayExpress  
12 (<https://www.ebi.ac.uk/arrayexpress/>)

1 **Acknowledgements:** This work was funded by ERC starting grant Relieve  
2 IMDs (LV, NRFH), the Cambridge Hospitals National Institute for Health  
3 Research Biomedical Research Center (LV, NRFH, SaS, FS.), the Evelyn  
4 trust (NH) and the EU Fp7 grant TissuGEN (MCDB) and supported in part by  
5 the Intramural Research Program of the NIH/NIAID (RLG, CAR). FS has been  
6 supported by an Addenbrooke's Charitable Trust Clinical Research Training  
7 Fellowship and a joint MRC-Sparks Clinical Research Training Fellowship.  
8 AWJ and AEM acknowledge the support from EPSRC (EP/L504920/1) and an  
9 Engineering for Clinical Practice Grant from the Department of Engineering,  
10 University of Cambridge. JB was supported by a BHF Studentship (Grant  
11 FS/13/65/30441).

12 The authors would like to thank J Skepper, L Carter and the University of  
13 Cambridge Advanced Imaging Centre for their help with electron microscopy;  
14 E Farnell and the University of Cambridge, Cambridge Genomic Services for  
15 their help with microarray data processing and analysis; A Petrunkina and the  
16 NIHR Cambridge BRC Cell Phenotyping Hub for their help with cell sorting; K  
17 Burling and the MRC MDU Mouse Biochemistry Laboratory  
18 [MRC\_MC\_UU\_12012/5] for processing mouse serum samples; R El-Khairi  
19 for her help with IF images, R Grandy for their help with providing relevant  
20 references, the Cambridge Biorepository for Translational Medicine for the  
21 provision of human tissue used in the study and Mr B McLeod for IT support.  
22 The monoclonal antibody TROMA-III developed by R Kemler was obtained  
23 from the Developmental Studies Hybridoma Bank, created by the NICHD of  
24 the NIH and maintained at The University of Iowa, Department of Biology,  
25 Iowa City, IA 52242.

1

2 **Author Contributions:** FS: Design and concept of study, execution of  
3 experiments and data acquisition, development of protocols and validation,  
4 collection and interpretation of data, production of figures, manuscript writing,  
5 editing and final approval of manuscript; AWJ: Conception of the technique,  
6 scaffold design and generation of densified collagen tubular scaffolds; OCT:  
7 animal experiments including kidney capsule injections; cell culture, provision  
8 and harvesting of mouse tissue; StS: Magnetic Resonance Imaging (MRI);  
9 EMG, SSU: MRI review and reporting; RLG: Animal experiments, IF, tissue  
10 histology; MCDB: Cell culture, generation of viral particles, viral transduction,  
11 generation of GMP-ECOs; NLB, LV: Animal experiments; MJGV, PM:  
12 Bioinformatics analyses; DO: Flow cytometry analyses; LY: Western blot  
13 analyses; AR: IF and QPCR analyses and provision of positive controls for IF  
14 and QPCR; AB: Flow cytometry analyses, bioinformatics support; JB: Tissue  
15 histology, IF; MarZ: Scaffold preparation; MTP: Generation of viral particles,  
16 viral transduction, generation of GMP-ECOs; MP: Generation of viral particles;  
17 GMS: scaffold generation; PMM,KES: maintenance and provision of fibroblast  
18 controls; NP: tissue culture; NG, CAR: Harvesting and preparation of primary  
19 tissue; IS: Karyotyping, CGH analyses; SD: Histology review and reporting;  
20 WS, JC, KBJ, MatZ, SaS, WTHG, GJA, SEB, TW, THK, EM: critical revision  
21 of the manuscript for important intellectual content. NRFH: Design and  
22 concept of study, early study supervision AEM: Scaffold design, critical  
23 revision of the manuscript for important intellectual content. KSP: Primary  
24 tissue provision, animal experiments, design and concept of study, study  
25 supervision, interpretation of data, editing and final approval of manuscript.

1 LV: Design and concept of study, study supervision, interpretation of data,  
2 editing and final approval of manuscript.

3

4 **Conflict of financial interests statement:** LV is a founder and shareholder  
5 of DefiniGEN. The remaining authors have nothing to disclose.

## References

1. Murray, K. F. & Carithers, R. L. AASLD practice guidelines: Evaluation of the patient for liver transplantation. *Hepatology* **41**, 1407–1432 (2005).
2. Perkins, J. D. Are we reporting the same thing?: Comments. *Liver Transplant.* **13**, 465–466 (2007).
3. Skaro, A. I. *et al.* The impact of ischemic cholangiopathy in liver transplantation using donors after cardiac death: The untold story. *Surgery* **146**, 543–553 (2009).
4. Enestvedt, C. K. *et al.* Biliary complications adversely affect patient and graft survival after liver retransplantation. *Liver Transpl.* **19**, 965–72 (2013).
5. Gallo, A. & Esquivel, C. O. Current options for management of biliary atresia. *Pediatr. Transplant.* **17**, 95–98 (2013).
6. Felder, S. I. *et al.* Hepaticojejunostomy using short-limb Roux-en-Y reconstruction. *JAMA Surg* **148**, 253–7-8 (2013).
7. Sampaziotis, F., Segeritz, C.-P. & Vallier, L. Potential of human induced pluripotent stem cells in studies of liver disease. *Hepatology* **62**, 303–311 (2015).
8. Kanno, N., LeSage, G., Glaser, S., Alvaro, D. & Alpini, G. Functional heterogeneity of the intrahepatic biliary epithelium. *Hepatology* **31**, 555–61 (2000).
9. Sampaziotis, F. *et al.* Cholangiocytes derived from human induced



- 1 pluripotent stem cells for disease modeling and drug validation. *Nat.*  
2 *Biotechnol.* 1–11 (2015). doi:10.1038/nbt.3275
- 3 10. Sampaziotis, F. *et al.* Directed differentiation of human induced  
4 pluripotent stem cells into functional cholangiocyte-like cells. *Nat.*  
5 *Protoc.* **12**, 814–827 (2017).
- 6 11. LeSage, G., Glaser, S. & Alpini, G. Regulation of cholangiocyte  
7 proliferation. *Liver* **21**, 73–80 (2001).
- 8 12. Huch, M. *et al.* Long-Term Culture of Genome-Stable Bipotent Stem  
9 Cells from Adult Human Liver. *Cell* **160**, 299–312 (2014).
- 10 13. Masyuk, A. I., Masyuk, T. V & LaRusso, N. F. Cholangiocyte primary  
11 cilia in liver health and disease. *Dev. Dyn.* **237**, 2007–12 (2008).
- 12 14. Tabibian, J. H., Masyuk, A. I., Masyuk, T. V., O'Hara, S. P. & LaRusso,  
13 N. F. Physiology of cholangiocytes. *Compr. Physiol.* **3**, 541–565 (2013).
- 14 15. Cízková, D., Morký, J., Micuda, S., Osterreicher, J. & Martínková, J.  
15 Expression of MRP2 and MDR1 transporters and other hepatic markers  
16 in rat and human liver and in WRL 68 cell line. *Physiol. Res.* **54**, 419–28  
17 (2005).
- 18 16. Gigliozi, A. *et al.* Molecular identification and functional  
19 characterization of Mdr1a in rat cholangiocytes. *Gastroenterology* **119**,  
20 1113–22 (2000).
- 21 17. Xia, X., Francis, H., Glaser, S., Alpini, G. & LeSage, G. Bile acid  
22 interactions with cholangiocytes. *World J. Gastroenterol.* **12**, 3553–63  
23 (2006).

- 1 18. Caperna, T. J., Blomberg, L. A., Garrett, W. M. & Talbot, N. C. Culture  
2 of porcine hepatocytes or bile duct epithelial cells by inductive serum-  
3 free media. *In Vitro Cell. Dev. Biol. Anim.* **47**, 218–33 (2011).
- 4 19. Marinelli, R. A. *et al.* Secretin induces the apical insertion of aquaporin-  
5 1 water channels in rat cholangiocytes. *Am. J. Physiol.* **276**, G280-6  
6 (1999).
- 7 20. Gong, A.-Y. *et al.* Somatostatin stimulates ductal bile absorption and  
8 inhibits ductal bile secretion in mice via SSTR2 on cholangiocytes. *Am.*  
9 *J. Physiol. Cell Physiol.* **284**, C1205-14 (2003).
- 10 21. Ito, M. *et al.* NOD/SCID/gamma(c)(null) mouse: an excellent recipient  
11 mouse model for engraftment of human cells. *Blood* **100**, 3175–82  
12 (2002).
- 13 22. Chan, B. P. & Leong, K. W. Scaffolding in tissue engineering: general  
14 approaches and tissue-specific considerations. *Eur. Spine J.* **17**, 467–  
15 479 (2008).
- 16 23. Cheung, H.-Y., Lau, K.-T., Lu, T.-P. & Hui, D. A critical review on  
17 polymer-based bio-engineered materials for scaffold development.  
18 *Compos. Part B Eng.* **38**, 291–300 (2007).
- 19 24. Jabłonska, B. End-to-end ductal anastomosis in biliary reconstruction:  
20 indications and limitations. *Can. J. Surg.* **57**, 271–277 (2014).
- 21 25. Gjorevski, N. *et al.* Designer matrices for intestinal stem cell and  
22 organoid culture. *Nature* **539**, 560–564 (2016).
- 23 26. Koo, B. K. & Clevers, H. Stem cells marked by the r-spondin receptor

- 1 LGR5. *Gastroenterology* **147**, 289–302 (2014).
- 2 27. Farin, H. F., Van Es, J. H. & Clevers, H. Redundant sources of Wnt  
3 regulate intestinal stem cells and promote formation of paneth cells.  
4 *Gastroenterology* **143**, 1518–1529.e7 (2012).
- 5
- 6

## 1 **Figure Legends**

2

### 3 **Figure 1**

4 Derivation and characterization of Extrahepatic Cholangiocyte Organoids  
5 (ECOs). **(a)** Schematic representation of the method used for the derivation of  
6 ECOs. **(b)** Quantitative real time PCR (QPCR) confirming the expression of  
7 biliary markers in Passage 1 (P1), Passage 10 (P10) and Passage 20 (P20)  
8 ECOs compared to freshly isolated Primary Cholangiocytes (PC) and  
9 Embryonic Stem (ES) cells used as a negative control, n=4 ECO lines.  
10 Center line, median; box, interquartile range (IQR); whiskers, range (minimum  
11 to maximum). Values are relative to the housekeeping gene  
12 Hydroxymethylbilane Synthase (*HMBS*) **(c)** Immunofluorescence (IF)  
13 analyses confirming the expression of biliary markers in ECO organoids.  
14 Scale bars: 100  $\mu$ m. Single channel and higher magnification images are  
15 provided in Supplementary Fig 3. **(d)** Euclidean hierarchical clustering  
16 analysis comparing the transcriptome of primary cholangiocytes (Primary),  
17 passage 20 ECOs (ECO), hIPSC-derived intrahepatic cholangiocyte-like-cells  
18 (iChoLC), ES cells (ES) and hepatocytes (HEP). For each probe, standard  
19 scores (z-scores) indicate the differential expression measured in number of  
20 standard deviations from the average level across all the samples. Clusters of  
21 genes expressed in ECOs, primary cholangiocytes or both cell types are  
22 indicated. GO analyses for each cluster are provided in Supplementary Fig  
23 7e. The data corresponds to 3 ECO lines.

24

## Figure 2

Functional characterization of ECO organoids. **(a)** Fluorescence images demonstrating secretion of the MDR1 fluorescent substrate rhodamine 123 in the lumen of ECOs, which is inhibited by the MDR1 inhibitor verapamil. Scale bars: 100  $\mu$ m. **(b)** Fluorescence intensity along the white line in **(a)**. **(c)** Mean intraluminal fluorescence intensity normalized to background in freshly plated Primary Cholangiocytes (Rho PC), Passage 20 ECOs (Rho P20) and P20 ECOs treated with verapamil (Ver). Error bars, Standard Deviation (SD); n=1565 measurements in total. Asterisks (\*\*\*\*) indicate statistical significance ( $P<0.001$ , Kruskal-Wallis test with Dunn's correction for multiple comparisons). **(d)** Luminal extrusion of the fluorescent bile acid CLF compared to controls loaded with FITC, confirming bile acid transfer. Scale bars: 100  $\mu$ m. **(e)** Fluorescence intensity along the white line in **(d)**. **(f)** Mean intra-luminal fluorescence intensity normalized over background, n=1947 total measurements. Error bars, SD; asterisks as in **(c)**. **(g)** ALP staining of ECOs. Scale bars: Light microscopy: 500  $\mu$ m, Whole well images: 1 cm. **(h)** Mean GGT activity of P20 ECOs vs. PCs; error bars, SD; n=3, asterisks as in **(c)**; one-way ANOVA with Dunnett's correction for multiple comparisons. **(i,j)** Mean diameter measurements **(i)** and live images **(j)** of ECOs treated with secretin or secretin and somatostatin, n=8. Error bars, SD; \*\*\* $P<0.001$ ; # $P>0.05$  (Kruskal-Wallis test with Dunn's correction for multiple comparisons). **(a-j)** Data representative of 3 different experiments.

## Figure 3

1 ECOs dissociated to single cells (ECO-SCs) can populate biodegradable PGA  
2 scaffolds. **(a,b)** Photographs of a PGA scaffold before **(a)** and after **(b)**  
3 treatment with ECOs. Scale bars: 1 cm. **(c)** Light microscopy images of a  
4 PGA scaffold populated with ECO-SCs. Red arrowheads: Fully populated  
5 scaffold; black arrowheads: cells recruiting new PGA fibers; white  
6 arrowheads: PGA fibers. Scale bars: 100µm. **(d)** Confocal microscopy images  
7 demonstrating cell expansion at different time-points after seeding of GFP-  
8 positive ECO-SCs on a PGA scaffold. White lines indicate the position of PGA  
9 fibers. Scale bars: 100µm. **(e)** IF demonstrating the expression of biliary  
10 markers and lack of EMT markers in ECO-SCs seeded on PGA scaffolds.  
11 Scale bars: 100 µm **(f)** QPCR analyses demonstrating the expression of  
12 biliary markers in ECOs before (ECOs) and after (scaffold) seeding on PGA  
13 scaffolds, n=4 ECO lines. Center line, median; box, interquartile range (IQR);  
14 whiskers, range (minimum to maximum). Values are relative to the  
15 housekeeping gene *HMBS*. **(g)** Mean ratio of CK7+/CK19+ and  
16 CK19+/Vimentin (VIM)+ cells in IF analyses similar to the image shown in **(e)**.  
17 Error bars represent SD; n=6. \*\* $P<0.01$  (Mann-Whitney test). **(h)** Mean GGT  
18 activity of ECO-SCs populating a PGA scaffold, n=4. Error bars represent SD.  
19 \*\*\*\* $P<0.001$  (two-tailed t-test). **(i)** ALP staining of PGA scaffolds populated by  
20 ECO-SCs. Scale bars: 500µm.

21

## 22 **Figure 4**

23 Biliary reconstruction in an extrahepatic biliary injury (EHBI) mouse model  
24 using ECOs. **(a)** Schematic representation of the method used for biliary

1 reconstruction. **(b)** Kaplan–Meier survival analysis, demonstrating rescue of  
 2 EHBI mice following biliary reconstruction with ECO-populated scaffolds.  
 3 **\*\* $P < 0.01$**  (log-rank test). **(c)** Images of gallbladders reconstructed with  
 4 acellular PGA scaffolds (scaffold only), PGA scaffolds populated with ECOs  
 5 (transplanted) and native un-reconstructed gallbladder controls (not  
 6 transplanted), demonstrating full reconstruction with ECO populated scaffolds.  
 7 CD: cystic duct, CBD: common bile duct, CHD: common hepatic duct, F:  
 8 fundus, A: anterior surface, P: posterior surface. Scale bars: 500  $\mu\text{m}$ . **(d)** H&E  
 9 staining of the reconstructed gallbladders. L: lumen. Scale bars: 100  $\mu\text{m}$  **(e)** IF  
 10 analyses demonstrating the presence of GFP-positive ECOs expressing  
 11 biliary markers in the reconstructed gallbladders. L: lumen Scale bars: 100  
 12  $\mu\text{m}$ . Higher magnification images are provided in Supplementary Fig 12 **(f,g)**  
 13 FITC cholangiogram (n=1) **(f)** and MRCP images (n=2) **(g)** of reconstructed  
 14 (transplanted) vs. native control (not transplanted) gallbladders (GB)  
 15 demonstrating a patent lumen and unobstructed communication with the rest  
 16 of the biliary tree. Scale bars: 1 mm.

17

## 18 **Figure 5**

19 ECOs can populate densified collagen tubular scaffolds. **(a)** Schematic  
 20 representation of the method used for the generation of densified collagen  
 21 tubular scaffolds. **(b)** Image of a densified collagen construct prior to tube  
 22 excision. Scale bar, 500  $\mu\text{m}$ . **(c)** Maximum intensity projection image  
 23 demonstrating a GFP+ ECO-populated tube after its generation. Scale bar; 30  
 24  $\mu\text{m}$  **(d)** Confocal microscopy image demonstrating lumen patency of an ECO-

1 populated collagen tube. Scale bar; 30  $\mu$ m. **(e)** Images of a near confluent  
2 GFP+ ECO-tube. Scale bar; 100  $\mu$ m. **(f)** IF analyses demonstrating the  
3 expression of biliary markers by ECOs following the generation of ECO-tubes.  
4 Scale bar; 100  $\mu$ m. **(g)** QPCR analyses demonstrating the expression of  
5 biliary markers before (ECOs) and after (Scaffold) the generation of ECO-  
6 populated collagen tubes. ES cells are used as a negative control, n=4 ECO  
7 lines. Center line, median; box, interquartile range (IQR); whiskers, range  
8 (minimum to maximum). Values are relative to *HMBS* expression. **(h, i)** ECO-  
9 tubes exhibit ALP **(h)** and GGT **(i)** activity. Scale bars, 500 $\mu$ m; MEFs, Mouse  
10 Embryonic feeders used as negative control; Scaffold, ECO-populated,  
11 densified collagen tubes; error bars, SD; n=3.

12

### 13 **Figure 6**

14 Bile duct replacement using ECO-populated densified collagen tubes. **(a)**  
15 Schematic representation of the method used. **(b)** Postmortem images of  
16 mice receiving ECO-populated collagen tubes (ECOs) vs. mice receiving  
17 fibroblast-populated tubes (fibroblasts). Bile flow results in yellow  
18 pigmentation of ECO-tubes. The white color of the fibroblast conduit  
19 combined with a dilated bile-filled (yellow color) Proximal Bile Duct (PBD)  
20 suggests luminal occlusion, resulting in bile leak (yellow peritoneal  
21 pigmentation; white dashed line). SC: Collagen tubes/scaffolds; DBD: Distal  
22 Bile Duct; scale bars 500  $\mu$ m. **(c)** Images of a thin walled construct resembling  
23 the native bile duct in animals receiving ECO-populated tubes vs. a thickened  
24 construct with no distinguishable lumen in animals receiving fibroblast tubes.



1 Scale bars 500  $\mu\text{m}$ . **(d)** QPCR using human-specific primers confirming the  
2 expression of biliary markers by transplanted ECO-populated tubes (ECOs in  
3 vivo) compared to cultured ECOs (ECOs in vitro) and mouse biliary tissue  
4 used as a negative control, n=4 **technical replicates**. Center line, median; box,  
5 interquartile range (IQR); whiskers, range (minimum to maximum). Values are  
6 relative to *HMBS* expression. **(e)** H&E staining demonstrating the presence of  
7 a biliary epithelium and a patent lumen in ECO-tubes but not fibroblast  
8 constructs. Scale bars 100  $\mu\text{m}$ . **(f)** IF analyses demonstrating a GFP+/ CK19+  
9 epithelium lining the lumen of ECO-constructs, vs. obliteration of the lumen by  
10 fibroblasts in fibroblast constructs. Scale bars 100  $\mu\text{m}$ . **(g)** FITC  
11 cholangiogram, demonstrating lumen patency in ECO-tubes vs. lumen  
12 occlusion in fibro-constructs. Scale bars: ECO, 100  $\mu\text{m}$ ; Fibroblasts, 500  $\mu\text{m}$   
13 **(h)** ALP activity is observed only in ECO-tubes, but not in fibroblast  
14 constructs. Scale bars: ECO, 100  $\mu\text{m}$ ; Fibroblasts, 500  $\mu\text{m}$ .

15

## 1    **Online Methods**

### 2    **Primary biliary tissue**

3    Primary biliary tissue (bile duct or gallbladder) was obtained from deceased  
4    organ donors from whom organs were being retrieved for transplantation. The  
5    gallbladder or a section of the bile duct was excised during the organ retrieval  
6    operation after obtaining informed consent from the donor's family (REC  
7    reference numbers: 12/EE/0253, NRES Committee East of England -  
8    Cambridge Central and 15/EE/0152 NRES Committee East of England -  
9    Cambridge South).

### 10   **Isolation of primary cholangiocytes**

11   Excised bile duct segments were placed in a 10 cm plate and washed once  
12   with William's E medium (Gibco, Life Technologies). A longitudinal incision  
13   was made along the wall of the excised bile duct segment exposing the lumen  
14   and 10-15 ml of William's E medium were added to cover the tissue. The  
15   luminal epithelium was subsequently scraped off using a surgical blade, while  
16   submerged in medium. The supernatant was collected and the tissue and  
17   plate were washed 2-3 times with William's E medium to harvest any  
18   remaining cells. The supernatant and washes were centrifuged at 444g for 4  
19   minutes. The pellet was washed with William's E, re-centrifuged and the  
20   supernatant was discarded (Figure 1a).

21   Excised gallbladders were placed in a 15 cm plate, a longitudinal incision was  
22   made along the wall of the excised gallbladder and the lumen was washed  
23   once with William's E medium (Gibco, Life Technologies). Cholangiocytes

1 were isolated and harvested following the method described above  
2 (Supplementary Fig 3a).

3 For isolation through brushings, an excised bile duct segment was placed in a  
4 10 cm plate and cannulated using an ERCP brush. The lumen was brushed  
5 10-20 times and the cells were harvested by washing the brush several times  
6 in a falcon tube containing 40-50 ml of William's E medium (Supplementary  
7 Fig 3b).

## 8 **Generation and culture of ECOs**

9 Isolated primary cholangiocytes were centrifuged at 444g for 4 minutes and  
10 re-suspended in a mixture of 66% matrigel (BD Biosciences, catalogue  
11 number: 356237) and 33% William's E medium (Gibco, Life Technologies)  
12 supplemented with 10mM nicotinamide (Sigma-Aldrich), 17mM sodium  
13 bicarbonate (Sigma Aldrich), 0.2mM 2-Phospho-L-ascorbic acid trisodium salt  
14 (Sigma-Aldrich), 6.3mM sodium pyruvate (Invitrogen), 14mM glucose (Sigma-  
15 Aldrich), 20mM HEPES (Invitrogen), ITS+ premix (BD Biosciences), 0.1µM  
16 dexamethasone (R&D Systems), 2mM Glutamax (Invitrogen), 100U/ml  
17 penicillin per 100µg/ml streptomycin, 20ng/ml EGF (R&D Systems), 500ng/ml  
18 R-Spondin (R&D Systems) and 100ng/ml DKK-1 (R&D Systems). The cell  
19 suspension was plated in 24-well plate format, at 50µl/well, so that a small  
20 dome of matrigel was formed in the centre of each well and then incubated at  
21 37°C for 10-30 minutes until it solidified. Subsequently, 1ml of William's E  
22 medium with supplements was added. The culture medium was changed  
23 every 48 hours.

1 To split the cells, the matrigel was digested by adding Cell Recovery Solution  
2 (Corning) for 30 minutes at 4°C. The resulting cell suspension was harvested,  
3 centrifuged at 444g for 4 minutes, washed once with William's E medium and  
4 re-suspended in 66% matrigel and 33% William's E medium with  
5 supplements, as described above.

6 All experiments were performed using passage 20 ECOs unless otherwise  
7 stated.

### 8 **Cell line identity**

9 Demographic data for donor corresponding to the each ECO lines is provided  
10 in supplementary table 1. Following derivation ECO lines were authenticated  
11 by matching their karyotype (Supplementary Fig. 4b) to the sex of the donor of  
12 origin. The lines were tested on a regular basis and found to be negative for  
13 mycoplasma contamination.

### 14 **Immunofluorescence, RNA extraction and Quantitative Real Time PCR**

15 IF, RNA extraction and QPCR were performed as previously described<sup>9</sup>. A  
16 complete list of the primary and secondary antibodies used is provided in  
17 supplementary table 3. A complete list of the primers used is provided in  
18 supplementary table 4.

19 All QPCR data are presented as the median, interquartile range (IQR) and  
20 range (minimum to maximum) of four independent ECO lines unless  
21 otherwise stated. Values are relative to the housekeeping gene  
22 Hydroxymethylbilane Synthase (*HMBS*).

23 All IF images were acquired using a Zeiss Axiovert 200M inverted microscope  
24 or a Zeiss LSM 700 confocal microscope. Imagej 1.48k software (Wayne

1 Rasband, NIHR, USA, <http://imagej.nih.gov/ij>) was used for image processing.  
2 IF images are representative of 3 different experiments. IF images of  
3 reconstructed gallbladder sections are representative of 5 different animals.

#### 4 **Microarrays**

65 RNA for microarray analysis was collected from 3 different ECO lines (n=3).  
66 The RNA was assessed for concentration and quality using a SpectroStar  
67 (BMG Labtech, Aylesbury, UK) and a Bioanalyser (Agilent Technologies,  
68 Cheadle, UK). Microarray experiments were performed at Cambridge  
69 Genomic Services, University of Cambridge, using the HumanHT-12 v4  
70 Expression BeadChip (Illumina, Chesterford, UK) according to the  
71 manufacturer's instructions. Briefly, 200ng of Total RNA underwent linear  
72 amplification using the Illumina TotalPrep RNA Amplification Kit (Life  
73 Technologies, Paisley, UK) following the manufacturer's instructions. The  
74 concentration, purity and integrity of the resulting cRNA were measured by  
75 SpectroStar and Bioanalyser. Finally cRNA was hybridised to the HumanHT-  
76 12 v4 BeadChip overnight followed by washing, staining and scanning using  
77 the Bead Array Reader (Illumina). The microarray data are available on  
78 ArrayExpress (Accession number: E-MTAB-4591). For reviewer access,  
79 please use the following login details Username: Reviewer\_E-MTAB-4591  
80 Password: rtlImbi0

#### 81 **Microarrays analysis**

82 Raw data was loaded into R using the lumi package from bioconductor<sup>28</sup> and  
83 divided into subsets according to the groups being compared; only the  
84 samples involved in a given comparison are used. Subsets were then filtered  
85 to remove any non-expressed probes using the detection p-value from

1 Illumina. Across all samples probes for which the intensity values were not  
2 statistically significantly different ( $P>0.01$ ) from the negative controls were  
3 removed from the analysis. Following filtering the data was transformed using  
4 the Variance Stabilization Transformation<sup>29</sup> from lumi and then normalised to  
5 remove technical variation between arrays using quantile normalisation.  
6 Comparisons were performed using the limma package<sup>30</sup> with results  
7 corrected for multiple testing using False Discovery Rate (FDR) correction.  
8 Finally the quality of the data was assessed along with the correlations  
9 between samples within groups.

10 Probes differentially expressed between HEP and ECOs representing the  
11 aggregate transcriptional “signature” of ECOs were selected for Euclidean  
12 hierarchical clustering using Perseus software (MaxQuant). Standard scores  
13 (z-scores) of the log2 normalized probe expression values across the different  
14 conditions were calculated and used for this analysis. Heatmaps and Primary  
15 Component Analysis (PCA) plots were generated using the MaxQuant  
16 Perseus software (<http://www.perseus-framework.org/>)<sup>31</sup>. Functional  
17 annotation and gene ontology analyses were performed on the genes  
18 differentially expressed between PCs and ECOs (Figure 1d) using the  
19 NIAID/NIH Database for Annotation, Visualization and Integrated Discovery  
20 (DAVID) v6.8 (<https://david.ncifcrf.gov/>)<sup>32,33</sup>.

## 21 **Western Analysis**

22 Total protein was extracted with lysis buffer (50mM Tris pH 8, 150mM NaCl,  
23 0.1% SDS, 0.5% sodium deoxycholate, 1% Triton X-100 and protease and  
24 phosphatase inhibitors). Protein concentrations were determined by BCA  
25 Protein Assay Kit (Thermo Fisher Scientific) according to the manufacturer’s

1 instructions. Samples were prepared for Western blot by adding 1x NuPAGE  
2 LDS Sample Buffer with 1%  $\beta$ -mercaptoethanol and incubated for 5 minutes  
3 at 95°C. Protein (25  $\mu$ g) was separated by 4-12% NuPAGE Bis-Tris protein  
4 gels (Invitrogen) and transferred onto PVDF membranes (Bio-Rad). Proteins  
5 were detected by probing with antibodies specific to Phospho- $\beta$ -catenin  
6 (Ser33/37/Thr41) (Cell Signalling Technology), Active- $\beta$ -catenin (Millipore),  
7 Total- $\beta$ -catenin (R&D),  $\alpha$ -tubulin (Sigma) followed by incubation with  
8 horseradish peroxidase anti-mouse, anti-goat or anti-rabbit secondary  
9 antibodies. Membranes were developed using Pierce ECL Western blotting  
10 substrate (Thermo Scientific) according to the manufacturer's instructions.

#### 11 **Rho Kinase activity analyses**

12 Rho Kinase activity was measured using a commercially available kit (Cell  
13 Biolabs, STA-416) according to the manufacturer's instructions

#### 14 **Flow cytometry analyses**

15 ECO organoids were harvested using Cell Recovery Solution (Corning) for 30  
16 minutes at 4°C, centrifuged at 444g for 4 minutes and dissociated to single  
17 cells using TrypLE<sup>TM</sup> Express (Gibco). The cells were subsequently fixed  
18 using 4% PFA for 20 minutes at 4°C. Cell staining and flow cytometry  
19 analyses were performed as previously described<sup>9,34</sup>.

#### 20 **Karyotyping**

21 ECO organoids were harvested using Cell Recovery Solution (Corning),  
22 dissociated to single cells as described above, plated in gelatin coated plates  
23 and cultured using William's E medium with supplements. When the cells  
24 were sub-confluent, usually after 72hrs, the cultures were incubated for 3-4  
25 hours with William's E medium with supplements containing 0.1 $\mu$ g/ml

1 colcemid (Karyomax®, Gibco). The cells were then harvested using Trypsin-  
2 EDTA (0.05%) (Gibco) for 4-5 minutes at 37°C, centrifuged at 344g for 5  
3 minutes and re-suspended in 5mls of KCl hypotonic solution (0.055M). The  
4 suspension was re-centrifuged at 344g for 5 minutes, 2 mls of a 3:1 100%  
5 methanol:glacial acetic acid solution were added and slides were prepared as  
6 previously described<sup>35</sup>

### 7 **Comparative Genomic Hybridization analyses**

8 Genomic DNA was labeled using the BioPrime DNA Labeling Kit (Invitrogen),  
9 according to the manufacturer's instructions and samples were hybridised to  
10 Agilent Sureprint G3 unrestricted CGH ISCA 8x60K human genome arrays  
11 following the manufacturer's protocol, as previously described<sup>36</sup>. The data  
12 was analysed using the Agilent CytoGenomics Software.

### 13 **Rhodamine123 transport assay**

14 The Rhodamine 123 transport assay was performed as previously described<sup>9</sup>  
15 and images were acquired using a Zeiss LSM 700 confocal microscope.  
16 Fluorescence intensity was measured between the organoid interior and  
17 exterior and luminal fluorescence was normalized over the background of the  
18 extraluminal space. Each experiment was repeated in triplicate. Error bars  
19 represent SD.

### 20 **Cholyl-Lysyl-Fluorescein transport assay**

21 To achieve loading with Cholyl-Lysyl-Fluorescein (CLF, Corning  
22 Incorporated), ECO organoids were split in 5µM of CLF and incubated at 37°C  
23 for 30 minutes. Images were acquired using a Zeiss LSM 700 confocal  
24 microscope and fluorescence intensity was measured between the organoid  
25 interior and exterior as described for the Rhodamine 123 transport assay. To



1 demonstrate that the changes in CLF fluorescence intensity observed were  
2 secondary to active export of CLF from the organoid lumen, the experiment  
3 was repeated with 5 $\mu$ M of unconjugated Fluorescein Isothiocyanate (FITC)  
4 (Sigma-Aldrich) as a control. Fluorescence intensity measurements were  
5 performed as described for the Rhodamine 123 transport assay. Each  
6 experiment was repeated in triplicate. Error bars represent SD.

#### 7 **GGT activity**

8 GGT activity was measured in triplicate using the MaxDiscovery™ gamma-  
9 Glutamyl Transferase (GGT) Enzymatic Assay Kit (Bioo scientific) based on  
10 the manufacturer's instructions. Error bars represent SD.

#### 11 **Alkaline Phosphatase staining**

12 Alkaline phosphatase was carried out using the BCIP/NBT Color  
13 Development Substrate (5-bromo-4-chloro-3-indolyl-phosphate/nitro blue  
14 tetrazolium) (Promega) according to the manufacturer's instructions.

#### 15 **Response to Secretin and Somatostatin**

16 Responses to secretin and somatostatin were assessed as previously  
17 described<sup>9</sup>.

#### 18 **Generation of ECOs expressing Green Fluorescent Protein**

19 EGFP expressing VSV-G pseudotyped, recombinant HIV-1 lentiviral particles  
20 were produced with an optimized second generation packaging system by  
21 transient co-transfection of three plasmids into HEK 293T cells (ATCC CRL-  
22 11268). EGFP expression is under control of a core EF1 $\alpha$ -promoter. All  
23 plasmids were a gift from Didier Trono and obtained from addgene (pWPT-  
24 GFP #12255, psPAX2 #12260, pMD2.G, #12259). Viral infection of organoids  
25 was performed as previously described<sup>37</sup>. Infected ECOs were expanded for 2

1 passages, harvested as described above for flow cytometry analyses and cell  
2 sorting by flow cytometry for GFP positive cells was performed. GFP  
3 expressing single cells were plated using our standard plating method and  
4 cultured in William's E medium with supplements for 1-2 weeks until fully  
5 grown ECO organoids developed.

#### 6 **Generation of ECO populated PGA scaffolds**

7 1mm thick PolyGlycolic Acid (PGA) scaffolds with a density of 50mg/cc were  
8 used for all experiments. Prior to seeding cells, the PGA scaffolds were pre-  
9 treated with a 1M NaOH for 10-30 seconds washed 3 times, decontaminated  
10 in a 70% ethanol solution for 30 minutes and then air-dried for another 30  
11 minutes until all the ethanol had fully evaporated. All scaffolds were a gift from  
12 Dr Sanjay Sinha and obtained from Biomedical Structures (Biofelt).

13 ECOs were harvested and dissociated to single cells as previously described  
14 for flow cytometry analyses.  $5-10 \times 10^6$  cells were re-suspended in 100  $\mu$ l of  
15 William's E medium with supplements, seeded on a scaffold surface area of  
16  $1\text{cm}^2$  and incubated at  $37^\circ\text{C}$  for 30-60 minutes to allow the cells to attach to  
17 the scaffold. The scaffolds were placed in wells of a 24-well plate and  
18 checked at regular intervals during this period to ensure the medium did not  
19 evaporate. If necessary, 10-20  $\mu$ l of William's E medium with supplements  
20 were added. After 1 hour, 2-3 mls of William's E medium with supplements  
21 were added to the wells and the medium was changed twice weekly.

#### 22 **Generation of densified collagen tubes**

23 Densified collagen tubes were prepared using a novel approach. A 3D printed  
24 chamber was fabricated, consisting of a funnel piece and a base plate. A  
25 250 $\mu$ m thick metallic wire was mounted into the base plate and fed through

1 the centre of the funnel. Absorbent paper towels were compacted between  
2 the two 3D printed parts, which were then screwed together. 5 mg mL<sup>-1</sup>  
3 collagen gel solution, loaded with cells, was poured into the funnel and gelled  
4 at 37°C for 30 min. After that time, the screws were loosened and, by placing  
5 the 3D printed chambers at 37°C for 2-4h, water was drawn out of the  
6 collagen gel. A cell-loaded densified collagen tube was thus formed with a  
7 250µm lumen and a wall thickness of 30-100 µm, determined by the duration  
8 of the drying phase. Upon removal from the chamber, the tube was trimmed  
9 for excess collagen and cut to the required length.

#### 10 **Culture of Human Mammary Epithelial Cells (HMECs)**

11 HMECs and the required tissue culture consumables were purchased as a kit  
12 from Lonza (cat no. CC-2551B) and the cells were cultured according  
13 to the supplier's instructions

#### 14 **Animal experiments**

15 All animal experiments were performed in accordance with UK Home Office  
16 regulations (UK Home Office Project License numbers PPL 80/2638 and PPL  
17 70/8702). Immunodeficient NOD.Cg-Prkdc<sup>scid</sup> Il2rg<sup>tm1Wjl</sup>/SzJ (NSG) mice which  
18 lack B, T and NK lymphocytes<sup>38</sup> were bred in-house with food and water  
19 available ad libitum pre- and post-procedures. A mix of male and female  
20 animals were used, aged approximately 6-8 weeks. All the ECO-constructs  
21 used were populated with ECOs derived from the common bile duct.

#### 22 **Generation of Extra-Hepatic Biliary Injury (EHBI) mouse model**

23 To generate a model of extrahepatic biliary injury, midline laparotomy was  
24 performed and the gallbladder was first mobilized by dividing the ligamentous  
25 attachment connecting its fundus to the anterior abdominal wall under

1 isoflurane general anesthesia. A longitudinal incision was then made along  
2 2/3 of the length of the gallbladder, from the fundus towards Hartmann's  
3 pouch (neck of gallbladder).

#### 4 **Biliary reconstruction in EHBI mice**

5 To reconstruct the gallbladder, a scaffold section measuring approximately 1 x  
6 1 mm (seeded with ECOs or without ECOs in controls) was sutured as a  
7 'patch' to close the defect using 4 – 6 interrupted 10'0 non-absorbable nylon  
8 sutures under 40x magnification. The laparotomy was closed in two layers  
9 with continuous 5'0 absorbable Vicryl sutures. The animals were given  
10 buprenorphine (temgesic 0.1 mg/kg) analgesia as a bolus and observed every  
11 15 minutes in individual cages until fully recovered.

12 8 animals underwent biliary reconstruction using an ECO-populated scaffold.  
13 All animals survived up to 104 days without complications and were culled  
14 electively for further analyses. Two control experiments were performed,  
15 where the animals underwent biliary reconstruction using acellular scaffolds.  
16 Both animals died within 24 hours from bile leak, therefore no further control  
17 experiments were performed to minimize animal discomfort.

#### 18 **Bile duct replacement**

19 The native common bile duct was divided and a short segment excised. The  
20 populated densified collagen tube was anastomosed end-to-end, using  
21 interrupted 10'0 nylon sutures, between the divided proximal and distal  
22 common bile duct. A length of 5'0 nylon suture material (diameter 100 µm)  
23 was inserted into the collagen tube and fed into the proximal and distal  
24 common bile duct to ensure patency of the lumen during the anastomosis.  
25 After the anastomosis was complete, the 5'0 suture was pushed into the

1 duodenum through the distal bile duct and was removed through an incision in  
2 the duodenum, which was then closed with interrupted 10'0 nylon sutures.  
3 Lumen patency was assessed at the time of transplantation through light  
4 microscopy and cannulation of the lumen with a 5'0 non-absorbable suture.  
5 Transplantation was abandoned as futile in case of fully occluded tubes due  
6 to cell infiltration. These events were considered construct/tube failure rather  
7 than surgical complications and therefore were not censored in the survival  
8 analysis.

### 9 **Bile duct ligation**

10 C57BL/6 mice were purchased from The Jackson Laboratory (Bar Harbor,  
11 ME). The mice were housed and bred in a Minimal Disease Unit at the animal  
12 facility at Oslo University Hospital, Rikshospitalet, Oslo. All experiments were  
13 performed on male mice between 8 and 12 weeks of age. A median  
14 laparotomy was performed, the common bile duct exposed and ligated close  
15 to the junction of the hepatic bile ducts. Sham operated mice underwent the  
16 same procedure without ligation. Serum was harvested after 5 days. Alanine  
17 transaminase (ALT), aspartate transaminase (AST) and alkaline phosphatase  
18 (ALP) were measured in serum using an ADVIA 1800 (Siemens) at The  
19 Central Laboratory, Norwegian School of Veterinary Science. All animal  
20 experiments were approved by the Norwegian Food Safety Authority (project  
21 license no FOTS 8210/15) and all animals received human care in line with  
22 "Guide for the Care and Use of Laboratory Animals" (National Institutes of  
23 Health Publication, 8th Edition, 2011).

### 24 **Blood sample collection**

1 Blood was taken using a 23g needles directly from the inferior vena cava  
2 under terminal anaesthesia at the time the animals were electively culled and  
3 transferred into 1.5ml Eppendorf tubes for further processing.

#### 4 **Blood sample processing**

5 The blood samples were routinely processed by the University of Cambridge  
6 Core biochemical assay laboratory (CBAL). All of the sample analysis was  
7 performed on a Siemens Dimension EXL analyzer using reagents and assay  
8 protocols supplied by Siemens.

#### 9 **Light microscopy imaging**

10 Light microscopy images of excised reconstructed gallbladders were acquired  
11 using a Leica MZFLIII fluorescence dissecting microscope. The images are  
12 representative of 5 animals.

#### 13 **Cryosectioning and Histology**

14 Excised gallbladders were fixed in 4% PFA, immersed in sucrose solution  
15 overnight, mounted in optimal cutting temperature (OCT) compound and  
16 stored at -80°C until sectioning. Sections were cut to a thickness of 10µm  
17 using a cryostat microtome and mounted on microscopy slides for further  
18 analysis

#### 19 **Haematoxylin and Eosin (H&E) Staining**

20 H&E staining was performed using Sigma-Aldrich reagents according to the  
21 manufacturer's instructions. Briefly, tissue sections were hydrated, treated  
22 with Meyer's Haematoxylin solution for 5 minutes (Sigma-Aldrich), washed  
23 with warm tap water for 15 minutes, placed in distilled water for 30-60  
24 seconds and treated with eosin solution (Sigma-Aldrich) for 30-60 seconds.

1 The sections were subsequently dehydrated and mounted using the Eukitt®  
2 quick-hardening mounting medium (Sigma-Aldrich). Histology sections were  
3 reviewed by an independent histopathologist with a special interest in  
4 hepatobiliary histology (SD).

#### 5 **TUNEL assay**

6 The TUNEL assay was performed using a commercially available kit (abcam,  
7 ab66110) according to the manufacturer's instructions.

#### 8 **Fluorescein Isothiocyanate (FITC) cholangiography**

9 In situ FITC cholangiography was performed in sacrificed animals after  
10 dissection of the gallbladder free from the adherent liver lobes, but before  
11 surgical interruption of the extrahepatic biliary tree. The distal bile duct was  
12 cannulated with a 23½ gauge needle and FITC injected retrogradely into the  
13 gallbladder and images taken under a fluorescent microscope.

#### 14 **Magnetic Resonance Cholangio-Pancreatography (MRCP)**

15 Magnetic resonance cholangio-pancreatography was performed after sacrifice  
16 of the animals. MRCP was performed at 4.7T using a Bruker BioSpec 47/40  
17 system. A rapid acquisition with relaxation enhancement sequence was used  
18 with an echo train length of 40 echoes at 9.5ms intervals, a repetition time of  
19 1000ms, field of view  $5.84 \times 4.18 \times 4.18 \text{ cm}^3$  with a matrix of  $256 \times 180 \times 180$   
20 yielding an isotropic resolution of 230  $\mu\text{m}$ . The actively-decoupled four-  
21 channel mouse cardiac array provided by Bruker was used for imaging.

22 For the second mouse imaged, for higher signal to noise ratio to give  
23 improved visualisation of the biliary ducts a two-dimensional sequence was  
24 used with slightly varied parameters (24 spaced echoes at 11ms intervals to  
25 give an effective echo time of 110ms; repetition time 5741ms; matrix size of

1 256×256; field of view of 4.33×5.35cm<sup>2</sup> yielding a planar resolution of  
2 170×200μm<sup>2</sup>). Fifteen slices were acquired coronally through the liver and gall  
3 bladder with a thickness of 0.6mm. For this acquisition, a volume coil was  
4 used to reduce the impact of radiofrequency inhomogeneity.

5 To examine the biliary ducts and gall bladder, images were prepared by  
6 maximum intensity projections. Structural imaging to rule out neoplastic  
7 growths was performed using a T1-weighted 3D FLASH (fast low-angle shot)  
8 sequence with a flip angle of 25°, repetition time of 14ms and an echo time of  
9 7ms. The matrix was 512×256×256 with a field of view of 5.12×2.56×2.56cm<sup>3</sup>  
10 for a final isotropic resolution of 100 μm.

11 The MRCP images were reviewed by 2 independent radiologists with a  
12 special interest in hepatobiliary radiology (EMG, SU).

### 13 **Statistical analyses**

14 All statistical analyses were performed using GraphPad Prism 6. For small  
15 sample sizes where descriptive statistics are not appropriate, individual data  
16 points were plotted. For comparison between 2 mean values a 2-sided  
17 student's t-test was used to calculate statistical significance. The normal  
18 distribution of our values was confirmed using the D'Agostino & Pearson  
19 omnibus normality test where appropriate. Variance between samples was  
20 tested using the Brown-Forsythe test. For comparing multiple groups to a  
21 reference group one-way ANOVA with Dunnett correction for multiple  
22 comparisons was used between groups with equal variance, while the  
23 Kruskal-Wallis test with Dunn's correction for multiple comparisons was  
24 applied for groups with unequal variance. Survival was compared using log-  
25 rank (Mantel-Cox) tests. Where the number of replicates (n) is given this



1 refers to ECO lines or number of different animals unless otherwise stated.  
2 Further details of the statistical analyses performed are provided in  
3 Supplementary table 5.

4 For animal experiments, group sizes were estimated based on previous study  
5 variance. Final animal group sizes were chosen to allow elective culling at  
6 different time point while maintaining  $n > 4$  animals surviving past 30 days to  
7 ensure reproducibility. No statistical methods were used to calculate sample  
8 size. No formal randomization method was used to assign animals to study  
9 groups. However; littermate animals from a cage were randomly assigned to  
10 experimental or control groups by a technician not involved in the study. No  
11 animals were excluded from the analysis. No blinding was used when only  
12 one group of animals survived for radiology imaging. In cases, such as  
13 gallbladders reconstructed with fibroblasts vs. ECOs where more than one  
14 groups survived to be imaged, both radiologists reviewing the images (EG  
15 and SU) where blinded to the method of reconstruction.

16

## References

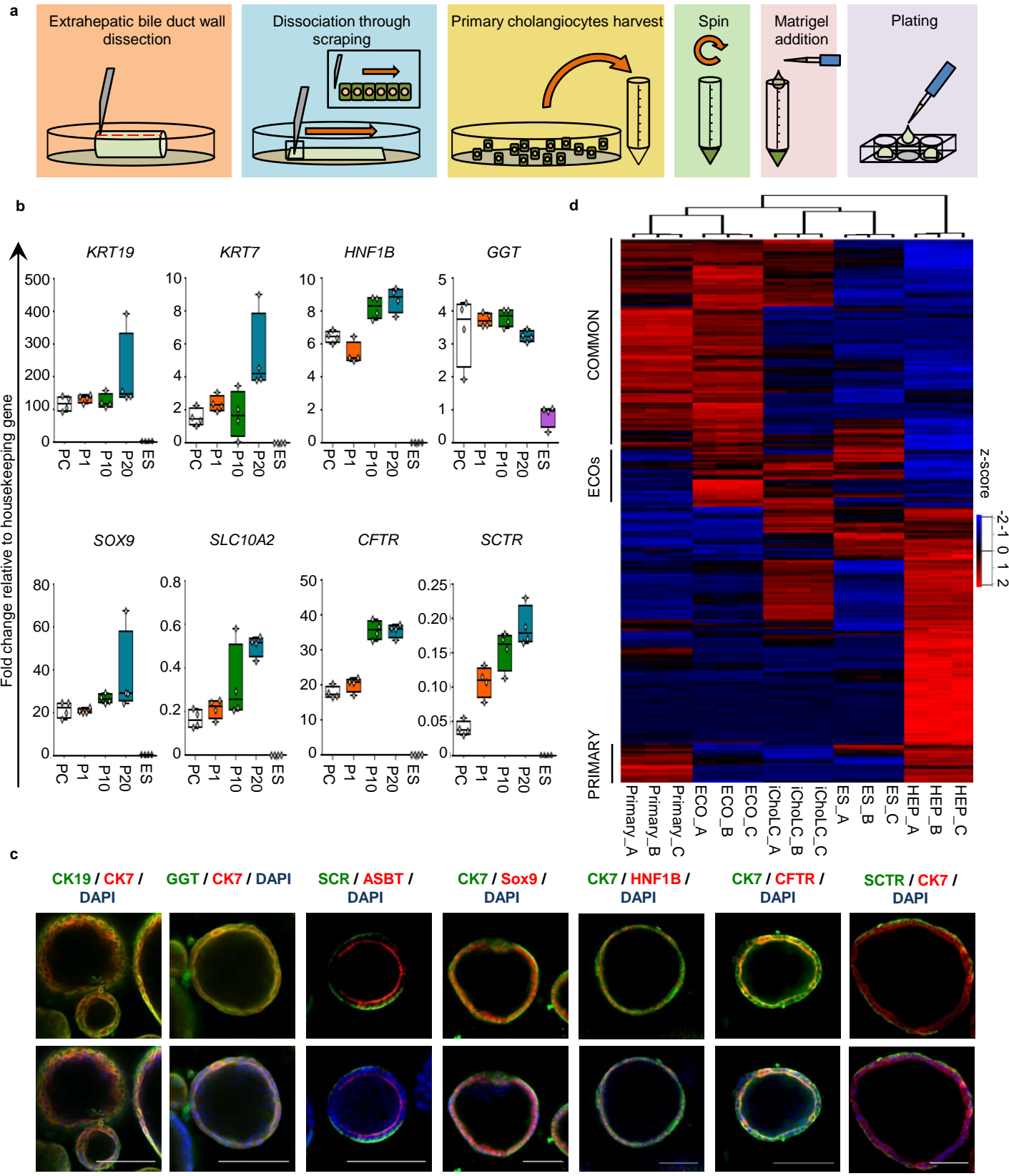
28. Du, P., Kibbe, W. a & Lin, S. M. lumi: a pipeline for processing Illumina microarray. *Bioinformatics* **24**, 1547–8 (2008).
29. Lin, S. M., Du, P., Huber, W. & Kibbe, W. A. Model-based variance-stabilizing transformation for Illumina microarray data. *Nucleic Acids Res.* **36**, (2008).
30. Smyth, G. K. Linear models and empirical bayes methods for assessing differential expression in microarray experiments. *Stat Appl Genet Mol Biol* **3**, Article3-Article3 (2004).
31. Tyanova, S. *et al.* The Perseus computational platform for comprehensive analysis of (prote)omics data. *Nat. Methods* **13**, 731–40 (2016).
32. Huang, D. W., Sherman, B. T. & Lempicki, R. A. Systematic and integrative analysis of large gene lists using DAVID bioinformatics resources. *Nat. Protoc.* **4**, 44–57 (2008).
33. Huang, D. W., Sherman, B. T. & Lempicki, R. A. Bioinformatics enrichment tools: paths toward the comprehensive functional analysis of large gene lists. *Nucleic Acids Res.* **37**, 1–13 (2009).
34. Bertero, A. *et al.* Activin/Nodal signaling and NANOG orchestrate human embryonic stem cell fate decisions by controlling the H3K4me3 chromatin mark. *Genes Dev.* **29**, 702–17 (2015).
35. Campos, P. B., Sartore, R. C., Abdalla, S. N. & Rehen, S. K. Chromosomal spread preparation of human embryonic stem cells for

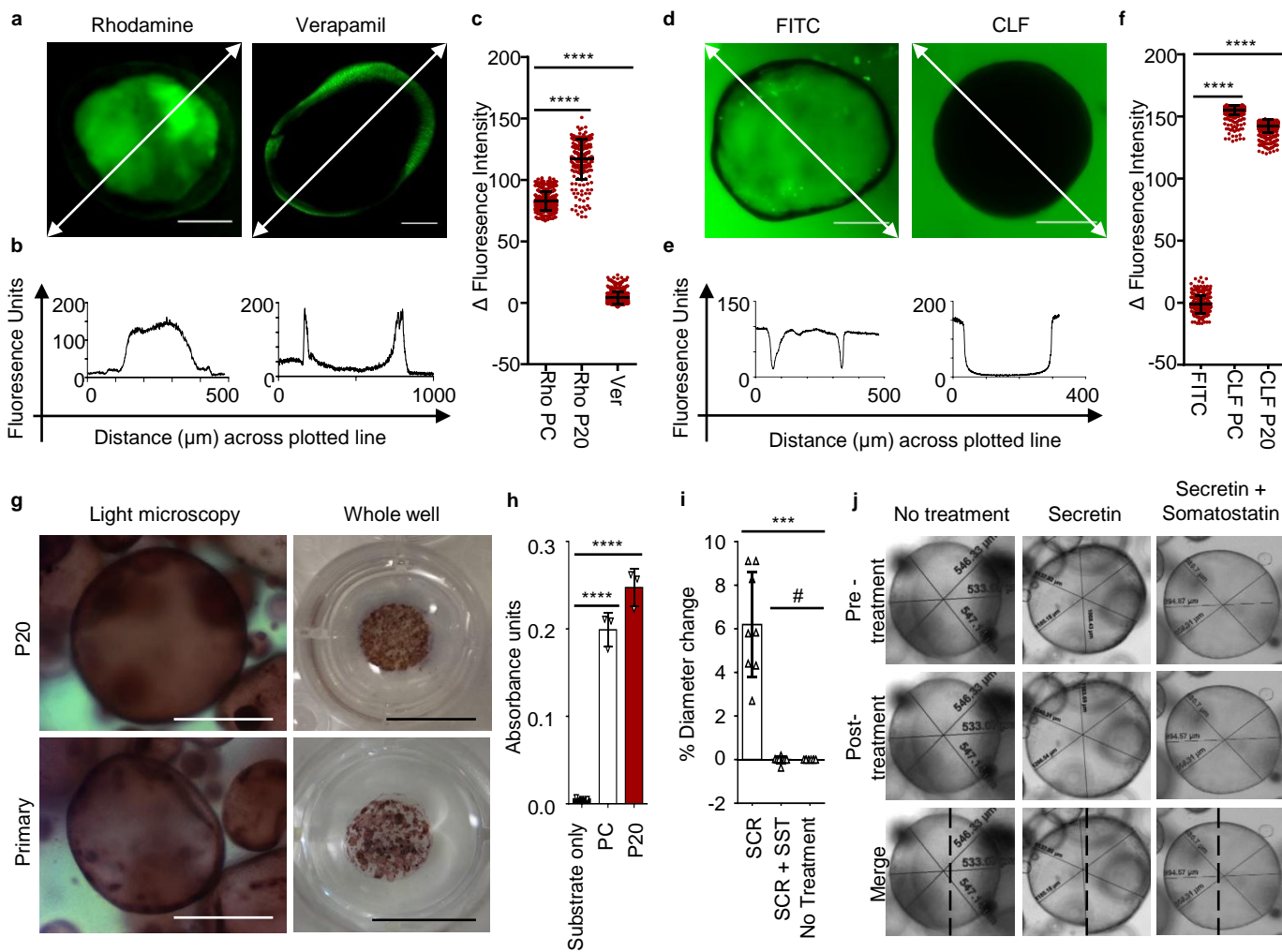
- 1 karyotyping. *J. Vis. Exp.* 4–7 (2009). doi:10.3791/1512
- 2 36. Hannan, N. R. F. *et al.* Generation of multipotent foregut stem cells from  
3 human pluripotent stem cells. *Stem Cell Reports* **1**, 293–306 (2013).
- 4 37. Koo, B.-K., Sasselli, V. & Clevers, H. Retroviral gene expression control  
5 in primary organoid cultures. *Curr. Protoc. Stem Cell Biol.* **27**, Unit 5A.6.  
6 (2013).
- 7 38. Shultz, L. D. *et al.* Human lymphoid and myeloid cell development in  
8 NOD/LtSz-scid IL2R gamma null mice engrafted with mobilized human  
9 hemopoietic stem cells. *J. Immunol.* **174**, 6477–6489 (2005).

10

11

12





Sampaziotis et al. Figure 3

